ISA Transactions 96 (2020) 185–194

Contents lists available at ScienceDirect

ISA Transactions

journal homepage: www.elsevier.com/locate/isatrans

Research article

Dynamic output feedback $\mathcal{H}_\infty$ design in finite-frequency domain for constrained linear systems

Ali Kazemy [a,*], Éva Gyurkovics [b], Tibor Takács [c]

[a] Department of Electrical Engineering, Tafresh University, Tafresh 39518-79611, Iran
[b] Mathematical Institute, Budapest University of Technology and Economics, 1111 Budapest, 3 Müegyetem rkp., Hungary
[c] Corvinus University of Budapest, 1093 Budapest, 8 Fővám tér, Hungary

HIGHLIGHTS

- Finite-frequency $\mathcal{H}_\infty$ control is designed for linear systems via dynamic output feedback.
- Practical hard constraints are considered in the design problem.
- The proposed method is effectively applied on the model of two practical structures.

ARTICLE INFO

Article history:
Received 8 September 2018
Received in revised form 3 June 2019
Accepted 4 June 2019
Available online 10 June 2019

Keywords:
Dynamic output feedback
Finite-frequency $\mathcal{H}_\infty$ control
gKYP lemma
$\mathcal{H}_\infty$ performance

ABSTRACT

This paper deals with the design problem of $\mathcal{H}_\infty$ control for linear systems in finite-frequency (FF) domain. Accordingly, the $\mathcal{H}_\infty$ norm from the exogenous disturbance to the controlled output is reduced in a given frequency range with utilizing the generalized Kalman–Yakubovic–Popov (gKYP) lemma. As some of the states are hard or impossible to measure in many applications, a dynamic output feedback controller is proposed. In order to meet practical requirements that express the limitations of the physical system and the actuator, these time-domain hard constraints are taken into account in the controller design. An algorithm terminating in finitely many steps is given to determine the dynamic output feedback with suboptimal FF $\mathcal{H}_\infty$ norm bound. The algorithm consists of solving a series of linear matrix inequalities (LMIs). Finally, two case studies are given to demonstrate the effectiveness and advantageous of the proposed method.

1. Introduction

The past few decades have witnessed remarkable developments in $\mathcal{H}_\infty$ control theory, which addresses the problem of worst-case controller design for systems subject to unknown external disturbances and uncertainties [1–4]. Particular attention has been paid to this subject in light of its robustness and disturbance attenuation capabilities. After the high-impact paper [2], a huge amount of papers has been devoted to theoretical and application sides of $\mathcal{H}_\infty$ theory [5–10], and to the implementation on many practical systems [11–19].

It is worth pointing out that the standard $\mathcal{H}_\infty$ control concerns the infinite-frequency range. However, in many real-world problems the signals of interest have a limited frequency spectrum: to mention but a few, the wave force for offshore platforms, earthquake force for multi-storey buildings and road disturbance for vehicles are signals of this kind. Therefore, it is important to investigate FF $\mathcal{H}_\infty$ control, because the consideration of a bounded frequency interval may reduce the conservatism of the standard $\mathcal{H}_\infty$ control. Fortunately, the gKYP lemma of [20] and [21] provides a way to optimize some infinite-frequency performances – including the $\mathcal{H}_\infty$ performance – in a FF range. With the aid of this method, the FF $\mathcal{H}_\infty$ control is developed and employed for many practical systems with promising results [15,22–26]. The advantage of FF $\mathcal{H}_\infty$ control in comparison with the entire-frequency $\mathcal{H}_\infty$ control is apparently illustrated in the paper [27].

On the one hand, the state-feedback control is probably the most common and most intensively investigated controller structure. This is because the state-feedback uses the internal information of the system to control it, which is generally much more informative than the system output. Therefore, many published papers on the FF $\mathcal{H}_\infty$ control have focused on state-feedback control [23,25,27]. On the other hand, output-feedback control has received great attention in the most important problems in control theory and applications due to the fact that all state variables are not always available for measurement. In this regard,

* Corresponding author.
E-mail addresses: kazemy@tafreshu.ac.ir (A. Kazemy), gye@math.bme.hu (É. Gyurkovics), takacs.tibor@uni-corvinus.hu (T. Takács).

https://doi.org/10.1016/j.isatra.2019.06.005
0019-0578/

the FF $\mathcal{H}_\infty$ static output-feedback control is developed and considered for active suspension systems [15], linear time-invariant fractional-order systems [28], and vibration control of structural systems [19]. Another kind of output-feedback controller is the dynamic output feedback controller. Theoretically, the dynamic output feedback controller is more powerful than a static output feedback controller while its design is more challenging [29,30]. To the best of our knowledge, there are only few results on $\mathcal{H}_\infty$ dynamic output feedback control over FF range with fixed $\mathcal{H}_\infty$-gain [29–31] limited to active vehicle suspension systems. Motivated by the aforementioned discussion, the aim of this paper is to design a FF $\mathcal{H}_\infty$ dynamic output feedback suboptimal controller for linear systems with practical constraints. The contributions of this paper can be mentioned as follows:

1. Finite-frequency $\mathcal{H}_\infty$ suboptimal control is designed for linear systems via dynamic output feedback.
2. Practical hard constraints are considered in the design problem.

Notation. Standard notations are used. Especially, $R > 0$ (≥ 0) stands for a real symmetric positive definite (semi-definite) matrix R, $\mathbf{S}_n$ and $\mathbf{S}_n^+$ denote the set of $n \times n$ symmetric and $n \times n$ symmetric and positive definite matrices, respectively. For a matrix R, its orthogonal complement is denoted by $R_\perp$, and $[R]_s = R + R^T$, $R^{-T} = (R^{-1})^T$. $\|T(s)\|_\infty$ represents the maximum singular value of a transfer-function matrix $T(s)$. A block-diagonal matrix is represented by diag{...} and a conjugate-transpose term in a Hermitian matrix is denoted by $*$.

2. Problem statement and preliminaries

Consider a linear dynamic system as

$$\begin{cases} \dot{x}(t) = A_x x(t) + B_x u(t) + E_x f(t), & x(0) = x_0, \\ z(t) = C_z x(t) + B_z u(t) + E_z f(t), \\ y(t) = C_y x(t), \\ v(t) = C_v x(t), \end{cases} \tag{1}$$

where $x(t) \in \mathbf{R}^{n_x}$ is the state vector, $z(t) \in \mathbf{R}^{n_z}$ represents the controlled or penalty output, $y(t) \in \mathbf{R}^{n_y}$ denotes the measured output vector, $v(t) \in \mathbf{R}^{n_v}$ is the output vector to be constrained, and $u(t) \in \mathbf{R}^{n_u}$ is the control signal. Function $f(t) \in \mathbf{L}_2[0, T)$ for any $T > 0$ is the external disturbance. The matrices $A_x \in \mathbf{R}^{n_x \times n_x}$, $B_x \in \mathbf{R}^{n_x \times n_u}$, $E_x \in \mathbf{R}^{n_x}$, $C_z \in \mathbf{R}^{n_z \times n_x}$, $B_z \in \mathbf{R}^{n_z \times n_u}$, $E_z \in \mathbf{R}^{n_z}$, $C_y \in \mathbf{R}^{n_y \times n_x}$ and $C_v \in \mathbf{R}^{n_v \times n_x}$ are known real matrices.

Due to practical requirements, some physical constraints are introduced for $v(t)$ and $u(t)$ as follows:

$$|v_i(t)| \leq 1, \quad i = 1, \ldots, n_v, \tag{2}$$

$$|u_j(t)| \leq u_{j,\max}, \quad j = 1, \ldots, n_u, \tag{3}$$

where the numbers $u_{j,\max}$ ($j = 1, \ldots, n_u$) are given constants.

Remark 1. Note that hard constraints for some state variables (or combinations of them) are necessary in several cases due to physical restrictions as it is shown in the examples of Section 4. For example, the state constraint in Example 1 means that the relative drifts of the floors of a building may not exceed a prescribed value. Similarly, due to the limitation in the maximum power of the actuator, the control signal should be constrained. The violation of the constraints may lead to damage to the structure or the actuator.

In order to simplify the formulation of forthcoming statements, the notion of admissible disturbances is introduced as follows. An external disturbance f satisfying inequality

$$\int_0^\infty f(t)^2 dt \leq f_{\max}^2 \tag{4}$$

with a given $f_{\max}$ is called *admissible*.

The dynamic output feedback controller is defined as

$$\begin{cases} \dot{\hat{x}}(t) = A_c \hat{x}(t) + B_c y(t), \\ u(t) = C_c \hat{x}(t) + D_c y(t), \end{cases} \tag{5}$$

where the matrices $A_c \in \mathbf{R}^{n_x \times n_x}$, $B_c \in \mathbf{R}^{n_x \times n_y}$, $C_c \in \mathbf{R}^{n_u \times n_x}$, and $D_c \in \mathbf{R}^{n_u \times n_y}$ are the controller gain matrices to be designed. For the sake of brevity, introduce the notation $\mathcal{K} = [A_c, B_c, C_c, D_c]$, which will also be referred to as the controller gain matrix.

Define $\xi(t) = \left[x^T(t), \hat{x}^T(t)\right]^T \in \mathbf{R}^{2n_x}$. Then, by substituting (5) into (1), one can obtain the closed-loop systems as

$$\begin{cases} \dot{\xi}(t) = \mathcal{A}\xi(t) + \mathcal{B}f(t), & \xi(0) = \xi_0 = [x_0^T, 0^T]^T, \\ \zeta(t) = \mathcal{C}\xi(t) + \mathcal{D}f(t), \end{cases} \tag{6}$$

where

$$\mathcal{A} = \begin{bmatrix} A_x + B_x D_c C_y & B_x C_c \\ B_c C_y & A_c \end{bmatrix}, \quad \mathcal{B} = \begin{bmatrix} E_x \\ 0 \end{bmatrix},$$
$$\mathcal{C} = \begin{bmatrix} C_z + B_z D_c C_y & B_z C_c \end{bmatrix}, \quad \mathcal{D} = E_z.$$

By introducing the notations $\kappa = \begin{bmatrix} D_c C_y & C_c \end{bmatrix}$, $\mathcal{C}_v = [C_v \; 0]$ and $e_j \in \mathbf{R}^{1 \times n_u}$ as the jth unit row vector (e.g. for $n_u = 4$, $e_2 = [0 \; 1 \; 0 \; 0]$), the constraints (2) and (3) can be written as

$$\xi^T(t) \mathcal{C}_{vi}^T \mathcal{C}_{vi} \xi(t) \leq 1, \quad i = 1, \ldots, n_v, \tag{7}$$

$$\xi^T(t) \kappa^T e_j^T e_j \kappa \xi(t) \leq u_{j,\max}^2, \quad j = 1, \ldots, n_u, \tag{8}$$

where $\mathcal{C}_{vi}$ is the ith row of $\mathcal{C}_v$. Note that $u_j(t) = e_j u(t)$. Consider the FF $\mathcal{H}_\infty$ performance index

$$\sup_{\varpi_1 < \omega < \varpi_2} \|\mathcal{G}(j\omega)\|_\infty < \gamma, \tag{9}$$

where ϖ_1 and ϖ_2 represent the lower and upper bound of the specified frequency, γ is a positive scalar, and $\mathcal{G}(j\omega)$ denotes the transfer-function matrix of the closed-loop system (6) from the exogenous disturbance $f(t)$ to the controlled output $\zeta(t)$. The problem statement can be formulated as the following.

Problem statement: The aim is to design a gain matrix $\mathcal{K} = [A_c, B_c, C_c, D_c]$ for the dynamic output feedback controller (5) such that,

- the closed-loop system (6) is asymptotically stable in case $f(t) = 0$,
- the FF $\mathcal{H}_\infty$ performance index (9) is assured with a γ as small as possible,
- the hard constraints (2) and (3) are met.

Remark 2. The basic tool for the construction of dynamic output feedback controller is the reduction of computations to matrix inequalities. As it is well-known, these matrix inequalities are bilinear in the decision variables. There are already available software tools (as e.g. PENLAB of Fiala, Kocvara & Stingl) for the solution of bilinear matrix inequalities (BMIs), but the applicability is limited in respect of the size of the problem. The standard method to reduce the BMI conditions to linear matrix inequalities (LMIs) originated from the seminal work of Gahinet–Apkarian [32] is suitable, if the $\mathcal{H}_\infty$ problem is considered on the entire-frequency domain. To eliminate the difficulties caused by *FF domain* and the *presence of hard constraints*, an iterative procedure will be proposed. It will be shown that the proposed method can efficiently be applied to practical problems presented in Section 4.

The following lemmas are utilized through the paper.

Lemma 1 (*Projection Lemma; [32,33]*). *Let matrices $A \in \mathbf{C}^{n\times m}$, $B \in \mathbf{C}^{k\times n}$ and $S = S^* \in \mathbf{C}^{n\times n}$ be given. Then the following statements are equivalent:*

(i) There exists a matrix Q satisfying

$$AQB + (AQB)^* + S < 0,$$

(ii) The following conditions hold:

$$A_\perp S A_\perp^* < 0 \qquad (or \quad AA^* > 0),$$
$$B_\perp^* S (B_\perp^*)^* < 0 \qquad (or \quad B^*B > 0).$$

Remark 3. It has to be emphasized that, even if $B \in \mathbf{R}^{n\times m}$, $C \in \mathbf{R}^{k\times n}$, *but* Q is complex Hermitian, equivalence of the two statements is valid only in the case, when X is allowed to be a general complex matrix, i.e. a nonzero imaginary part should be assumed, and no assumption on the structure of X should be stated. Otherwise, one only has (i) $\Rightarrow$ (ii).

Lemma 2 (*gKYP Lemma; [20,21]*). *Real matrices $A \in \mathbf{R}^{n\times n}$, $B \in \mathbf{R}^{n\times m}$, $C \in \mathbf{R}^{p\times n}$, $D \in \mathbf{R}^{p\times m}$, a real number $\gamma > 0$, and an interval $\mathcal{I}_\omega = \{\omega \in \mathbf{R} : \overline{\omega}_1 \le \omega \le \overline{\omega}_2\}$ are given. Let $\mathcal{G}(j\omega) = C(j\omega I - A)^{-1}B + D$. Suppose that A has no eigenvalues on the imaginary axis, and $D^TD - \gamma^2 I < 0$. Then the following statements are equivalent:*

(i) $\begin{bmatrix} \mathcal{G}(j\omega) \\ I \end{bmatrix}^* \Pi \begin{bmatrix} \mathcal{G}(j\omega) \\ I \end{bmatrix} < 0$, *for all* $\omega \in \mathcal{I}_\omega$.

(ii) There exist real symmetric matrices P and Q with $Q > 0$ such that

$$\begin{bmatrix} A & B \\ I & 0 \end{bmatrix}^T \Xi \begin{bmatrix} A & B \\ I & 0 \end{bmatrix} + \begin{bmatrix} C & D \\ 0 & I \end{bmatrix}^T \Pi \begin{bmatrix} C & D \\ 0 & I \end{bmatrix} < 0, \tag{10}$$

where $\Xi = \begin{bmatrix} -Q & P + j\omega_c Q \\ P - j\omega_c Q & -\overline{\omega}_1\overline{\omega}_2 Q \end{bmatrix}$, $\Pi = \begin{bmatrix} I & 0 \\ 0 & -\gamma^2 I \end{bmatrix}$, *and* $\omega_c = \frac{1}{2}(\overline{\omega}_1 + \overline{\omega}_2)$.

Corollary 1. *Under the conditions of Lemma 2, statement (i) of Lemma 2 is equivalent to the following:*

(iii) There exist real symmetric matrices P, Q with $Q > 0$, and real matrices W_r, W_{im} such that

$$\left[\begin{array}{cc} \widehat{\Omega}_r + j\widehat{\Omega}_{im} & \Gamma^T \\ \hline \Gamma & -I \end{array}\right] < 0, \tag{11}$$

where $\Gamma = [0\ C\ D]$,

$$\widehat{\Omega}_r = \begin{bmatrix} -Q & P - W_r & 0 \\ P - W_r^T & \Omega_{1r} & W_r^T B \\ 0 & B^T W_r & -\gamma^2 I \end{bmatrix},$$
$$\Omega_{1r} = A^T W_r + W_r^T A - \overline{\omega}_1\overline{\omega}_2 Q, \tag{12}$$

$$\widehat{\Omega}_{im} = \begin{bmatrix} 0 & \omega_c Q - W_{im} & 0 \\ -\omega_c Q + W_{im}^T & \Omega_{1im} & -W_{im}^T B \\ 0 & B^T W_{im} & 0 \end{bmatrix},$$
$$\Omega_{1im} = A^T W_{im} - W_{im}^T A. \tag{13}$$

Proof. The proof follows similar arguments as e.g. a part of the proof of Theorem 1 in [18]. By Lemma 2, statements (i) and (ii) are equivalent. Set

$$\widetilde{\Xi} = \left[\begin{array}{cc|c} & & 0 \\ \multicolumn{2}{c|}{\Xi} & 0 \\ \hline 0 & 0 & 0 \end{array}\right] + \left[\begin{array}{cc|c} 0 & 0 & 0 \\ 0 & C^TC & C^TD \\ \hline 0 & D^TC & D^TD - \gamma^2 I \end{array}\right].$$

Now inequality (10) can equivalently be written as

$$\begin{bmatrix} A & B \\ I & 0 \\ \hline 0 & I \end{bmatrix}^T \widetilde{\Xi} \begin{bmatrix} A & B \\ I & 0 \\ \hline 0 & I \end{bmatrix} < 0. \tag{14}$$

Since $Q > 0$ and $D^TD - \gamma^2 I < 0$ are assumed, inequality

$$\Theta_{1\perp}^T \widetilde{\Xi} \Theta_{1\perp} < 0, \tag{15}$$

holds true together with (14), where $\Theta_{1\perp} = \begin{bmatrix} I & 0 & 0 \\ 0 & 0 & I \end{bmatrix}$. Here $\Theta_{1\perp}$ is the orthogonal complement of $\Theta_1 = [0\ I\ 0]^T$. Using the notation $\Theta_2 = [-I\ A\ D]^T$, it can be seen that (14) is nothing else as $\Theta_{2\perp}^T \widetilde{\Xi} \Theta_{2\perp} < 0$. The application of Lemma 1 shows that (14) and (15) are equivalent to the existence of a matrix $\widehat{W} = W_r + jW_{im}$ such that

$$\widetilde{\Xi} + \Theta_2 \widehat{W} \Theta_1^T + \Theta_1 \widehat{W} \Theta_2^T < 0.$$

It can be shown that, by using Schur complements, (11) is equivalent to the above inequality. □

3. Main results

Firstly, the condition on $\mathcal{H}_\infty$-stability will be derived. Secondly, an algorithm terminating in finitely many steps will be given to determine the dynamic output feedback with the lowest $\mathcal{H}_\infty$-norm bound.

Proposition 1. *Let $\mathcal{I}_\omega = \{\omega \in \mathbf{R} : \overline{\omega}_1 \le \omega \le \overline{\omega}_2\}$ and let $\mathcal{G}(j\omega)$ be the transfer function matrix of system (6). Suppose that $\mathcal{A}$ has no eigenvalues on the imaginary axis, and $\gamma > 0$ is such a number that $\mathcal{D}^T\mathcal{D} - \gamma^2 I < 0$. Then*

$$\sup_{\omega\in\mathcal{I}_\omega} \|\mathcal{G}(j\omega)\|_\infty < \gamma, \tag{16}$$

if and only if there exist matrices $\mathcal{P} \in \mathbf{S}_{2n_x}$, $\mathcal{Q} \in \mathbf{S}_{2n_x}^+$, $\mathcal{W}_r, \mathcal{W}_{im} \in \mathbf{R}^{2n_x\times 2n_x}$ such that the following matrix inequality holds:

$$\left[\begin{array}{cc|cc} \widehat{\Omega}_r & \Gamma^T & \widehat{\Omega}_{im} & 0 \\ \Gamma & -I & 0 & 0 \\ \hline -\widehat{\Omega}_{im} & 0 & \widehat{\Omega}_r & \Gamma^T \\ 0 & 0 & \Gamma & -I \end{array}\right] < 0, \tag{17}$$

where Γ, $\widehat{\Omega}_r$, $\widehat{\Omega}_{im}$ are obtained from (iii) of Lemma 2 with $[A, B, C, D] = [\mathcal{A}, \mathcal{B}, \mathcal{C}, \mathcal{D}]$, $P = \mathcal{P}$, $Q = \mathcal{Q}$, $W_r = \mathcal{W}_r$, $W_{im} = \mathcal{W}_{im}$.

Proof. The proof immediately follows from Corollary 1 by using the well-known fact that the Hermitian matrix $S = S_1 + jS_2$ is negative definite if and only if the real symmetric matrix $\begin{bmatrix} S_1 & S_2 \\ -S_2 & S_1 \end{bmatrix}$ is negative definite, as well. □

Remark 4. Divide the selectable variables in inequality (17) into two groups: let the first one be defined by $\Psi_0 = [\mathcal{P}, \mathcal{Q}, \mathcal{W}_r, \mathcal{W}_{im}, \overline{\gamma}]$, where $\overline{\gamma} = \gamma^2$, and the second one by $\mathcal{K} = [A_c, B_c, C_c, D_c]$. Formally, inequality (17) can be written as

$$\mathcal{L}_0(\Psi_0, \mathcal{K}) < 0, \tag{18}$$

which is LMI with respect to the decision variables in Ψ_0 by fixing the matrices in $\mathcal{K}$, and it is LMI with respect to the decision variables in $\mathcal{K}$ by fixing the parameters in Ψ_0.

For given $\mathcal{R} \in \mathbf{S}_{2n_x}^+$ and $\alpha > 0$, introduce the ellipsoid

$$\mathcal{E}_\alpha(\mathcal{R}) = \left\{\xi \in \mathbf{R}^{2n_x} : \xi^T \mathcal{R} \xi \le \alpha\right\}.$$

Proposition 2. *Let $\alpha_0 > 0$, $\nu > 0$ be given, and consider system (6) with admissible disturbances compliant with (4). Suppose that there exists a matrix $\mathcal{R} \in \mathbf{S}^+_{2n_x}$ such that the following matrix inequalities hold true:*

$$\begin{bmatrix} \mathcal{A}^T\mathcal{R} + \mathcal{R}\mathcal{A} & \mathcal{B}^T\mathcal{R} \\ \mathcal{R}\mathcal{B} & -\nu I \end{bmatrix} < 0, \tag{19}$$

$$\begin{bmatrix} \mathcal{R} & \overline{\alpha}\kappa^T e_j^T/\sqrt{u_{j,max}} \\ \overline{\alpha}e_j\kappa/\sqrt{u_{j,max}} & \overline{\alpha}u_{j,max} \end{bmatrix} \geq 0, \qquad j = 1, \ldots, n_u, \tag{20}$$

$$\begin{bmatrix} \mathcal{R} & \overline{\alpha}\mathcal{C}_{v_i}^T \\ \overline{\alpha}\mathcal{C}_{v_i} & \overline{\alpha} \end{bmatrix} q \geq 0, \qquad i = 1, \ldots, n_v, \tag{21}$$

where $\overline{\alpha} = \alpha_0 + \nu f_{max}^2$. Then

- *system (6) is asymptotically stable in case $f(t) = 0$,*
- *if f is an admissible disturbance and $\xi_0 = \left[x_0^T, 0^T\right]^T \in \mathcal{E}_{\alpha_0}(\mathcal{R})$, then $\xi(t) \in \mathcal{E}_{\overline{\alpha}}(\mathcal{R})$ for all $t \geq 0$, and the constraints (2) and (3) are satisfied.*

Proof. Let $V(\xi(t)) = \xi^T(t)\mathcal{R}\xi(t)$. It can be shown in a standard way that (19) implies inequality

$$\frac{d}{dt}V(\xi(t)) - \nu f^T(t)f(t) < 0. \tag{22}$$

Then,

$$V(\xi(\tau)) - V(\xi(0)) < \nu \int_0^\tau f^T(t)f(t)dt. \tag{23}$$

For $f(t) \equiv 0$, (22) implies that $\frac{d}{dt}V(\xi(t)) < 0$, thus the internal stability follows. For disturbances satisfying (4) one has

$$V(\xi(\tau)) \leq V(\xi(0)) + \nu f_{\max}^2,$$

therefore for any initial condition satisfying $\xi_0 \in \mathcal{E}_{\alpha_0}(\mathcal{R})$, one obtains that

$$\xi(\tau)^T\mathcal{R}\xi(\tau) \leq \alpha_0 + \nu f_{\max}^2 = \overline{\alpha},$$

i.e. $\xi(t) \in \mathcal{E}_{\overline{\alpha}}(\mathcal{R})$ for all $t \geq 0$. Consider now $u_j(t) = e_j\kappa\xi(t)$, $j = 1, \ldots, n_u$. It can be seen in a standard way that

$$\begin{bmatrix} u_{j,\max}^2\mathcal{R} & \kappa^T e_j{}^T \\ e_j\kappa & \frac{1}{\overline{\alpha}} \end{bmatrix} \geq 0, \qquad j = 1, \ldots, n_u, \tag{24}$$

implies (8), thus (3) as well. A simple congruence transformation shows that (24) is equivalent to (20). One can prove in a similar way that (21) implies (7) and (2). This completes the proof. □

Remark 5. The selectable variables of (19)–(21) can be divided into two groups analogously to Remark 4 to see that matrix inequalities (19), (20) and (21) are bilinear with respect to the decision variables $\Psi_1 = [\mathcal{R}, \nu]$ and $\mathcal{K} = [A_c, B_c, C_c, D_c]$. Formally, one can write these inequalities as

$$\mathcal{L}_1(\Psi_1, \mathcal{K}) < 0, \qquad \mathcal{L}_2(\Psi_1, \mathcal{K}) \geq 0, \qquad \mathcal{L}_3(\Psi_1, \mathcal{K}) \geq 0, \tag{25}$$

which are LMIs with respect to the decision variables in Ψ_1 by fixing the matrices in $\mathcal{K}$, and they are also LMIs with respect to the decision variables in $\mathcal{K}$ by fixing the parameters in Ψ_1.

Remarks 4 and 5 suggest the following idea: if there is a suitable guess for (A_c, B_c, C_c, D_c), then one can reduce γ by iteratively solving the obtained bilinear inequalities alternately fixing one or the other group of the decision variables. How to obtain a suitable initial guess? If a γ_0 is fixed, one can seek the solution of the dynamic output feedback problem by solving the $\mathcal{H}_\infty$-problem on the *entire*-frequency domain $\omega \in \mathcal{R}$. If it has a feasible solution, then it is a feasible solution of the $\mathcal{H}_\infty$-problem on the restricted frequency domain. The construction can be done by an approach frequently applied since [32].

To this end, several notations are needed. Let $\mathcal{R} \in \mathbf{S}^+_{2n_x}$, and

$$\mathcal{R} = \begin{bmatrix} X & N_1 \\ N_1^T & Z \end{bmatrix}, \quad \mathcal{R}^{-1} = \begin{bmatrix} Y & N_2 \\ N_2^T & W \end{bmatrix},$$
$$F_1 = \begin{bmatrix} X & I \\ N_1^T & 0 \end{bmatrix}, \quad F_2 = \begin{bmatrix} I & Y \\ 0 & N_2^T \end{bmatrix}. \tag{26}$$

Furthermore, define matrices

$$\widetilde{L} = N_1B_c + XB_xD_c, \quad \widetilde{K} = C_cN_2^T + D_cC_yY, \quad \widetilde{D} = D_c, \tag{27}$$

$$\widetilde{A} = XA_xY + \widetilde{L}C_yY + C_y^TD_c^TB_x^T + XB_xC_cN_2^T + N_1A_cN_2^T. \tag{28}$$

Proposition 3. *Let $\alpha_0 > 0$, $\overline{\gamma}_0 > 0$ be given, and consider system (1) with admissible disturbances compliant with (4). Suppose that there exist matrices $X, Y \in \mathbf{S}^+_{n_x}$, $\widetilde{A} \in \mathbf{R}^{n_x \times n_x}$, $\widetilde{L} \in \mathbf{R}^{n_x \times n_y}$, $\widetilde{K} \in \mathbf{R}^{n_u \times n_x}$, $\widetilde{D} \in \mathbf{R}^{n_u \times n_y}$ such that LMIs*

$$\Phi^0 = \begin{bmatrix} X & I \\ I & Y \end{bmatrix} > 0, \tag{29}$$

$$\Phi^1 = \begin{bmatrix} \Phi_{11}^1 & A_x^T + \widetilde{A} & XE_x & \Phi_{14}^1 \\ * & \Phi_{22}^1 & E_x & \Phi_{24}^1 \\ * & * & -\overline{\gamma}_0 I & E_z^T \\ * & * & * & -I \end{bmatrix} < 0, \tag{30}$$

$$\Phi_{11}^1 = XA_x + A_x^TX + \widetilde{L}C_y + C_y\widetilde{L}^T, \qquad \Phi_{14}^1 = C_z^T + C_y^T\widetilde{D}^TB_z^T,$$
$$\Phi_{22}^1 = A_xY + YA_x^T + B_x\widetilde{K} + \widetilde{K}^TB_x^T, \qquad \Phi_{24}^1 = YC_z^T + \widetilde{K}^TB_z^T,$$

$$\Phi_j^2 = \begin{bmatrix} X & I & \frac{1}{\sqrt{u_{j,max}}}C_y^T\widetilde{D}^Te_j^T \\ * & Y & \frac{1}{\sqrt{u_{j,max}}}\widetilde{K}^Te_j^T \\ * & * & u_{j,max}\,\mu \end{bmatrix} \geq 0, \qquad j = 1, \ldots, n_u, \tag{31}$$

$$\Phi_i^3 = \begin{bmatrix} X & I & C_{vi}^T \\ * & Y & YC_{vi}^T \\ * & * & \mu \end{bmatrix} \geq 0, \qquad i = 1, \ldots, n_v, \tag{32}$$

hold true, where $\mu = 1/\left(\alpha_0 + \overline{\gamma}_0 f_{max}^2\right)$. Let N_1, N_2 be defined by factorization $I - XY = N_1N_2^T$. Then matrices A_c, B_c, C_c, D_c obtained by subsequent solution of (27), (28) yield an internally stable closed-loop system (6), satisfying constraints (2), (3) and having the property

$$\mathcal{G}(j\omega)^*\,\mathcal{G}(j\omega) < \overline{\gamma}_0, \text{ for all } \omega \in \mathbf{R}. \tag{33}$$

Proof. Let $V(\xi(t)) = \xi(t)^T\mathcal{R}\xi(t)$. Then

$$\frac{d}{dt}V(\xi(t)) + \zeta(t)^T\zeta(t) - \overline{\gamma}_0 f(t)^Tf(t) = \begin{bmatrix} \xi(t) \\ f(t) \end{bmatrix}^T \Upsilon \begin{bmatrix} \xi(t) \\ f(t) \end{bmatrix},$$

where

$$\Upsilon = \begin{bmatrix} \mathcal{A}^T & I \\ \mathcal{B}^T & 0 \end{bmatrix}\begin{bmatrix} 0 & \mathcal{R} \\ \mathcal{R} & 0 \end{bmatrix}\begin{bmatrix} \mathcal{A} & \mathcal{B} \\ I & 0 \end{bmatrix} + \begin{bmatrix} \mathcal{C}^T & 0 \\ \mathcal{D}^T & I \end{bmatrix}\begin{bmatrix} I & 0 \\ 0 & -\overline{\gamma}_0 I \end{bmatrix}\begin{bmatrix} \mathcal{C} & \mathcal{D} \\ 0 & I \end{bmatrix}.$$

Thus $\Upsilon < 0$ implies that

$$V(\xi(T)) - V(\xi(0)) + \int_0^T \zeta(t)^T\zeta(t)dt < \overline{\gamma}_0 \int_0^T f(t)^Tf(t)dt, \tag{34}$$

which in turn implies the internal stability of (6) and property (33), provided that $\mathcal{R}$ is positive definite. However,

$$F_1^T\mathcal{R}^{-1}F_1 = \begin{bmatrix} X & I \\ I & Y \end{bmatrix}, \tag{35}$$

which is positive definite according to (29), thus $\mathcal{R}^{-1}$ and $\mathcal{R}$ are positive definite as well.

Using Schur complements, one can see that $\Upsilon < 0$ is equivalent to

$$\begin{bmatrix} \mathcal{R}\mathcal{A}+\mathcal{A}^T\mathcal{R} & \mathcal{R}\mathcal{B} & \mathcal{C}^T \\ \mathcal{B}^T\mathcal{R} & -\overline{\gamma}_0 I & \mathcal{D}^T \\ \mathcal{C} & \mathcal{D} & -I \end{bmatrix} < 0. \tag{36}$$

Taking a congruence transformation with diag $\left\{\mathcal{R}^{-1}F_1, I, I\right\}$, substituting the definition of $\mathcal{A}$, $\mathcal{B}$, $\mathcal{C}$, $\mathcal{D}$, Eqs. (27), (28), and taking into consideration that $\mathcal{R}^{-1}F_1 = F_2$, one can verify that (36) is equivalent to (30).

Next, the control and state constraints (7) and (8) have to be investigated. Because of (34), inclusion

$$\xi(t) \in \mathcal{E}_\mu(\mathcal{R}), \qquad t \geq 0 \tag{37}$$

holds true for any initial value $\xi_0 \in \mathcal{E}_{\alpha_0}(\mathcal{R})$. Therefore

$$\begin{bmatrix} \mathcal{R} & \mu\sqrt{u_{\mathrm{j,max}}}\kappa^T e_j^T \\ * & \mu u_{\mathrm{j,max}} \end{bmatrix} \geq 0, \quad j = 1, \ldots, n_u, \tag{38}$$

implies (8) provided that $\xi_0 \in \mathcal{E}_{\alpha_0}(\mathcal{R})$. Taking into consideration (35) and performing a congruence transformation with diag $\left\{\mathcal{R}^{-1}F_1, I\right\}$, one can verify that (38) is equivalent to (31). It can be seen from (37) in an analogous way that (32) implies (7).

Finally, it has to be shown that Eqs. (27)–(28) are solvable for D_c, C_c, B_c and A_c. Condition (29) implies that $I - XY$ is positive definite. Consider a factorization $I - XY = N_1N_2^T$, (e.g. by singular value decomposition or a QR factorization). Since matrices N_1 and N_2 are invertible, matrices D_c, C_c, B_c and A_c can be determined from Eqs. (27)–(28). This completes the proof. □

Algorithm

Step 0. Chose $\alpha_0 > 0$, $\overline{\gamma}_0 > 0$. Solve the system of LMIs (29)–(32) for the decision variables $X, Y, \widetilde{A}, \widetilde{K}, \widetilde{L}, \widetilde{D}$. If it has a feasible solution, then compute N_1, N_2 from $I - XY = N_1N_2^T$, $\mathcal{R}$ from (26), and A_c, B_c, C_c, D_c from (27), (28). Let $\overline{\gamma}^{(0)} = \overline{\gamma}_0$, $\mathcal{K}^{(0)} = \{A_c, B_c, C_c, D_c\}$, and $k = 1$. Choose some $\gamma_{\min} > 0$, and $N_{max} \in \mathbf{N}^+$.

Step k. (i) If $\mathcal{K}^{(k-1)}$ is known, solve problem P1 for Ψ_0, Ψ_1 :

$$\begin{aligned} P1: \quad & \min \ \overline{\gamma}, \quad \text{with respect to} \\ & \mathcal{L}_0\left(\Psi_0, \mathcal{K}^{(k-1)}\right) < 0, \quad \mathcal{L}_1\left(\Psi_1, \mathcal{K}^{(k-1)}\right) < 0, \\ & \mathcal{L}_2\left(\Psi_1, \mathcal{K}^{(k-1)}\right) \geq 0, \quad \mathcal{L}_3\left(\Psi_1, \mathcal{K}^{(k-1)}\right) \geq 0, \\ & \text{according to (18) and (25). Let} \Psi_0^{(k)}, \\ & \Psi_1^{(k)} \text{be defined as the solution.} \end{aligned}$$

(ii) If $\Psi_0^{(k)}$, $\Psi_1^{(k)}$ is known, solve problem P2 for $\mathcal{K}$ and $\varepsilon > 0$:

$$\begin{aligned} P2: \quad & \min(-\varepsilon), \quad \text{with respect to} \\ & \mathcal{L}_0\left(\Psi_0^{(k)}, \mathcal{K}\right) < -\varepsilon, \quad \mathcal{L}_1\left(\Psi_1^{(k)}, \mathcal{K}\right) < -\varepsilon, \\ & \mathcal{L}_2\left(\Psi_1^{(k)}, \mathcal{K}\right) \geq 0, \quad \mathcal{L}_3\left(\Psi_1^{(k)}, \mathcal{K}\right) \geq 0. \\ & \text{Let } \mathcal{K}^{(k)} \text{ be defined as the solution.} \end{aligned}$$

If $\overline{\gamma}^{(k-1)} > \overline{\gamma}^{(k)} > \gamma_{\min}$ and $k < N_{max}$, then set $k = k + 1$, and repeat step k, otherwise stop.

Theorem 1. *If the LMIs in Step 0 have a feasible solution, then problems P1 and P2 are feasible, Step k defines a strictly decreasing sequence $\overline{\gamma}^{(k)}$, and the algorithm terminates in finitely many steps yielding a suboptimal solution of the formulated problem.*

Proof. Suppose that Step 0 was successful. Then $\mathcal{K}^{(0)}$ defines a closed-loop system, which is internally asymptotically stable, the constraints are satisfied and

$$\sup_{\omega\in\mathbf{R}} \|\mathcal{G}(j\omega)\|_\infty^2 < \overline{\gamma}_0.$$

Consequently, in accordance with Corollary 1, there exists a solution of

$$\mathcal{L}_0\left(\Psi_0, \mathcal{K}^{(0)}\right) < 0,$$

if $\overline{\gamma} = \overline{\gamma}_0$ is taken. Furthermore, if $\overline{\mathcal{R}}$ is taken as $\mathcal{R}$ from the solution of Step 0, and $\overline{\nu}$ as $\nu = \overline{\gamma}_0$, then $\overline{\Psi}_1 = \left\{\overline{\mathcal{R}}, \overline{\nu}\right\}$ satisfies inequalities

$$\mathcal{L}_1\left(\overline{\Psi}_1, \mathcal{K}^{(0)}\right) < 0, \qquad \mathcal{L}_i\left(\overline{\Psi}_1, \mathcal{K}^{(0)}\right) \geq 0, \qquad i = 2, 3,$$

thus problem P1 is feasible. Let the solution be denoted by $\Psi_0^{(1)}$, $\Psi_1^{(1)}$, and the minimum value of $\overline{\gamma}$ by $\overline{\gamma}^{(1)}$. Because of the strict inequalities, there exists an $\overline{\varepsilon} > 0$ such that $\mathcal{L}_0\left(\Psi_0^{(1)}, \mathcal{K}^{(0)}\right) < -\overline{\varepsilon}$ and $\mathcal{L}_1\left(\Psi_1^{(1)}, \mathcal{K}^{(0)}\right) < -\overline{\varepsilon}$, while $\mathcal{L}_i\left(\Psi_1^{(1)}, \mathcal{K}^{(0)}\right) \geq 0$, $i = 2, 3$ remain valid. Thus problem P2 is feasible, too, and $\mathcal{K}^{(1)}$ is well-defined. Since $\overline{\gamma}^{(0)}$ belongs to the set of feasible solutions,

$$\overline{\gamma}^{(1)} \leq \overline{\gamma}^{(0)}$$

holds. If $\overline{\gamma}^{(1)} = \overline{\gamma}^{(0)}$ or $\overline{\gamma}^{(1)} \leq \gamma_{\min}$, then the algorithm terminates, and $\overline{\gamma}^{(1)}$, $\mathcal{K}^{(1)}$ yields the solution of our problem. Otherwise, the considerations above can be repeated inductively for $k = 2, 3 \ldots$ until either $\overline{\gamma}^{(k)} = \overline{\gamma}^{(k-1)}$ or $\overline{\gamma}^{(k)} \leq \gamma_{\min}$ or $k = N_{max}$ is satisfied. This completes the proof. □

Remark 6. The theorem states on the one hand that the LMIs preserve the feasibility in each step of the iteration, provided that the initial step was feasible. On the other hand, the iteration yields a strictly decreasing sequence $\overline{\gamma}^{(k)}$ until $\overline{\gamma}^{(k-1)} = \overline{\gamma}^{(k)}$, or the given lower bound $\overline{\gamma}_{\min}$ (or the given maximum number of iterations) is reached, thus a *suboptimal* solution is obtained. Observe that the LMIs to be solved are getting to be ill-posed near to the infimum value of $\overline{\gamma}$, thus it is advantageous to prescribe a $\overline{\gamma}_{\min}$ for computations because of numerical reasons.

4. Illustrative examples

The effectiveness of the proposed method will be illustrated by two case studies. The computations have been performed by MATLAB and YALMIP [34]. As it can be seen below, the parameters of both case studies are of significantly different magnitudes. Therefore, it was expedient to use an appropriate scaling before the computations in order to achieve numerical stability. However, the presented results are given in the original units.

Example 1. Consider a three-storey building model drawn in Fig. 1 [22]. In this model, all three storeys are supposed to be identical with masses, damping and stiffness coefficients equal to $m_i = 345.6$ ton, $c_i = 2973$ kN s/m^{-1}, and $k_i = 3.404 \times 10^5$ kN/m, $i = 1, 2, 3$, respectively. The symbol q_i stands for the relative drift between ith and $(i-1)$th floor, and $\ddot{x}_g = f(t)$ is the earthquake acceleration force. Define $q(t) = [q_1(t), q_2(t), q_3(t)]^T$ and $x(t) = [q^T(t), \dot{q}^T(t)]^T$. Based on the given parameters, the matrices in (1) are as follows (for more details about obtaining

these matrices see [22]):

$$A_x = \begin{bmatrix} 0 & 0 & 0 & 1 & 0 & 0 \\ 0 & 0 & 0 & 0 & 1 & 0 \\ 0 & 0 & 0 & 0 & 0 & 1 \\ -984.95 & 984.95 & 0 & -8.6 & 8.6 & 0 \\ 984.95 & -1969.9 & 984.95 & 8.6 & -17.2 & 8.6 \\ 0 & 984.95 & -1969.9 & 0 & 8.6 & -17.2 \end{bmatrix},$$

$$B_x = 10^{-6} \times \begin{bmatrix} 0 & 0 & 0 \\ 0 & 0 & 0 \\ 0 & 0 & 0 \\ 2.89 & 0 & 0 \\ -2.89 & 2.89 & 0 \\ 0 & -2.89 & 2.89 \end{bmatrix}, \quad E_x = \begin{bmatrix} 0 \\ 0 \\ 0 \\ -1 \\ 0 \\ 0 \end{bmatrix},$$

$$C_y = \begin{bmatrix} 0_{3\times3} & I_3 \end{bmatrix}, \quad C_v = \begin{bmatrix} \frac{1}{z_{\max}} \times I_3 & 0_{3\times3} \end{bmatrix},$$

$$C_z = \operatorname{diag}\{3, 1, 1, 3, 1, 1\},$$

and $B_z = 0_{6\times3}$, $E_z = 0_{6\times1}$. Parameter $z_{\max}$ is the maximum allowable relative drift between the floors and it is considered to be 2 cm (0.02 m). Note that the matrices C_y and C_z are taken from [18]. The 1940 El-Centro earthquake real data is utilized for the input disturbance $f(t)$, which is plotted in Fig. 2. It has been shown in [22] that the earthquakes happen in frequency range equal to 0.3–8.8 Hz, i.e. $\varpi_1 = 0.3$ and $\varpi_2 = 8.8$. For such a system with the given parameters, the controller gain matrices are obtained after two iterations as

$$A_c = \begin{bmatrix} 2194 & 2495.2 & 1707.3 & 12116 & -6063.8 & 11104 \\ -2101.9 & -782.94 & -1424.3 & -10485 & 19621 & -1760.9 \\ -1130.6 & -903.92 & 4.5845 & -218.79 & -18762 & -11722 \\ -1335.3 & 1058.8 & -280.52 & -420.06 & 463.73 & -1463.1 \\ 619.32 & -1863.4 & 1788.9 & 73.87 & -892.89 & 200.45 \\ -10.757 & -321.7 & 351.18 & 110.29 & 98.148 & -1210 \end{bmatrix},$$

$$B_c = 10^{6} \times \begin{bmatrix} 1.5284 & 4.6307 & -0.92638 \\ -0.95314 & 6.2436 & 0.27299 \\ -0.5147 & 4.3993 & 1.4704 \\ -0.098311 & 18.017 & -3.4045 \\ 0.014268 & -16.537 & 23.131 \\ -0.034514 & -1.8597 & 4.7301 \end{bmatrix},$$

$$D_c = \begin{bmatrix} -2749.6 & -1430 & -438.88 \\ -2169.8 & -1914.3 & -698.64 \\ -2036.3 & -1844.9 & -1323.8 \end{bmatrix},$$

$$C_c = \begin{bmatrix} -2.5824 & -2.9097 & -2.1788 & 5.7761 & 15.046 & -66.202 \\ -1.6189 & -2.1792 & -1.5 & 10.521 & 9.8605 & -61.777 \\ -1.4117 & -1.8261 & -1.5665 & 10.294 & 16.943 & -58.249 \end{bmatrix}$$

with the minimum value $\overline{\gamma} = 2.2890 \times 10^{-6}$. The closed-loop response of the relative drifts to 1940 El-Centro earthquake is shown in Fig. 3. It is clear that the maximum drifts are much smaller than $z_{\max} = 2$ cm (20 mm), so the constraints are met. In order to illustrate the effectiveness of the proposed controller, three articles, [19,22] and [18], are opted to compare the results. The papers [22] and [19] are devoted to the design of state-feedback and static-output-feedback FF $\mathcal{H}_\infty$ control, respectively, while paper [18] presents a dynamic output feedback controller. Although the methods used in these papers are different and they have different fields of applicability, their performance on control of buildings can correctly be compared with each other. Since an important characteristic of the performance is γ, indicating the effect of the disturbance to the controlled output, the obtained value of it is reported in Table 1 for each controller. Note that the method presented in [18] used a given value of γ, but the other papers, including this paper, calculated it by an optimization procedure. Obviously, the proposed controller has been able to

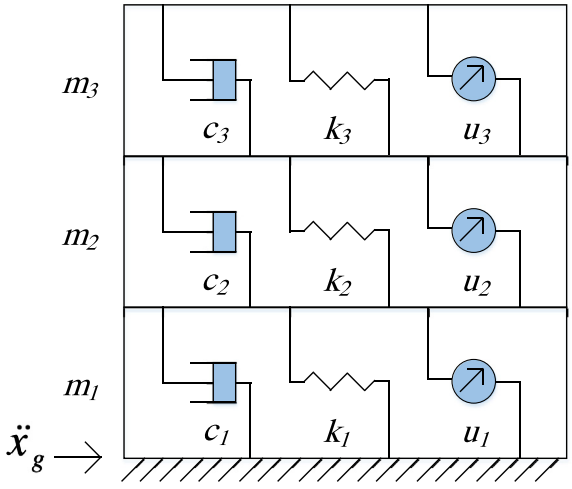

Fig. 1. A three-storey building model [22].

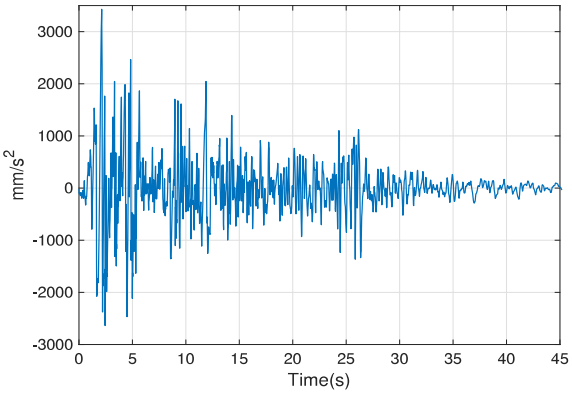

Fig. 2. The 1940 El-Centro earthquake real data for the input disturbance $f(t)$.

Table 1
Minimum obtained performance level (γ_{min}) for different controllers.

Controller	γ_{min}
FF $\mathcal{H}_\infty$ state feedback controller in [22]	0.0166
Dynamic output feedback controller in [18]	0.0086
FF $\mathcal{H}_\infty$ static output feedback controller in [19]	0.0038
The proposed controller	0.0015

achieve a lower minimum performance level than the other controllers. For simulating the results, all these controllers including the proposed controller are applied to the building model and the resulted relative drifts of the first, the second, and the third floors to 1940 El-Centro earthquake are plotted in Figs. 4, 5, and 6, respectively. These figures demonstrate that the qualitative behaviour of the relative drifts is much better for the proposed controller than the others. The only exception is the behaviour of the third floor under the application of the controller proposed by [19]. Since the peak values of relative drifts are very important, these values for each floor are compared in Fig. 7(a). At the same time, Fig. 7(b) illustrates that the peak of control signal of the proposed method is not significantly increased compared to other methods (less than 10%).

Example 2. In this example, an offshore steel jacket platform is considered, which has been discussed in many papers [13,35–37]. This platform is equipped with an active mass damper (AMD). A simplified model of this platform is drawn in Fig. 8,

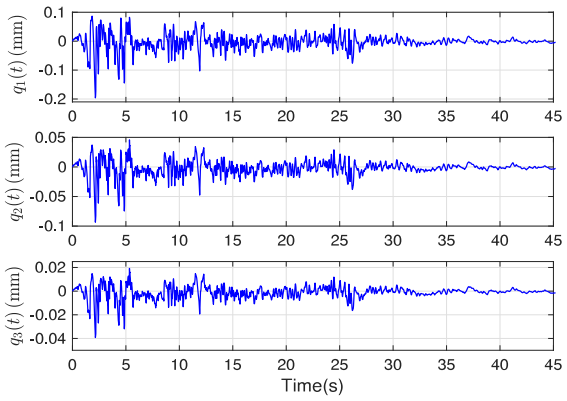

Fig. 3. Relative drifts of the floors to 1940 El-Centro earthquake.

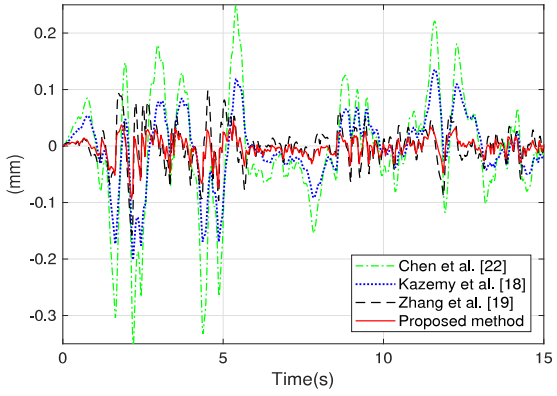

Fig. 4. Relative drift of the first floor to 1940 El-Centro earthquake.

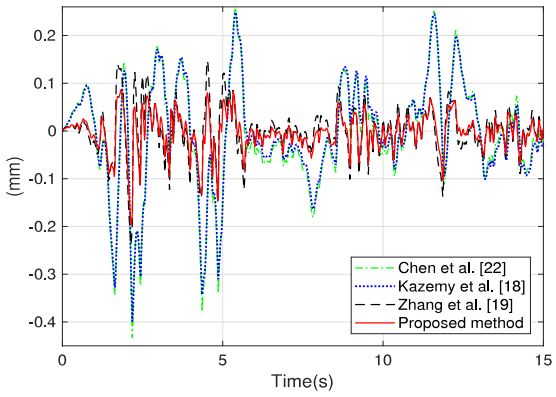

Fig. 5. Relative drift of the second floor to 1940 El-Centro earthquake.

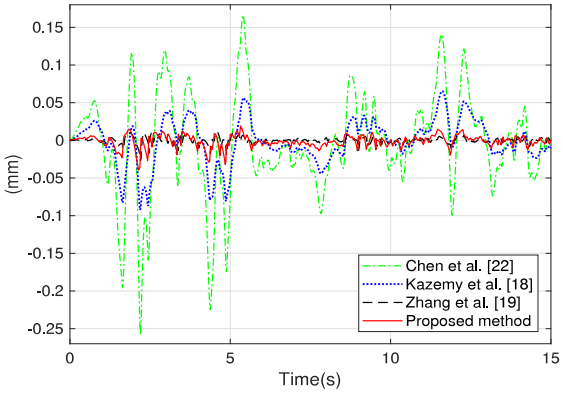

Fig. 6. Relative drift of the third floor to 1940 El-Centro earthquake.

where $z_p(t)$ and $z_a(t)$ denote the displacements of the platform deck and the AMD, respectively, $f(t)$ is the external wave force from the sea, and $u(t)$ is the control signal. Define $x(t) = [x_1(t), x_2(t), x_3(t), x_4(t)]^T = [z_p(t), z_a(t), \dot{z}_p(t), \dot{z}_a(t)]^T$. Based on the parameters given in [35], the following matrices are obtained:

$$A_x = \begin{bmatrix} 0 & 0 & 1 & 0 \\ 0 & 0 & 0 & 1 \\ -4.2290 & 0.0403 & -0.0899 & 0.0080 \\ 4.0297 & -4.0297 & 0.8030 & -0.8030 \end{bmatrix},$$

$$B_x = 10^{-4} \times \begin{bmatrix} 0 \\ 0 \\ -0.0013 \\ 0.1278 \end{bmatrix}, \quad E_x = 10^{-6} \times \begin{bmatrix} 0 \\ 0 \\ 0.1278 \\ 0 \end{bmatrix},$$

$$C_z = \begin{bmatrix} 1 & 0 & 0 & 0 \\ -4.2290 & 0.0403 & -0.0899 & 0.0080 \end{bmatrix},$$

$$B_z = 10^{-4} \times \begin{bmatrix} 0 \\ -0.0013 \end{bmatrix}, \quad E_z = 10^{-6} \times \begin{bmatrix} 0 \\ 0.1278 \end{bmatrix},$$

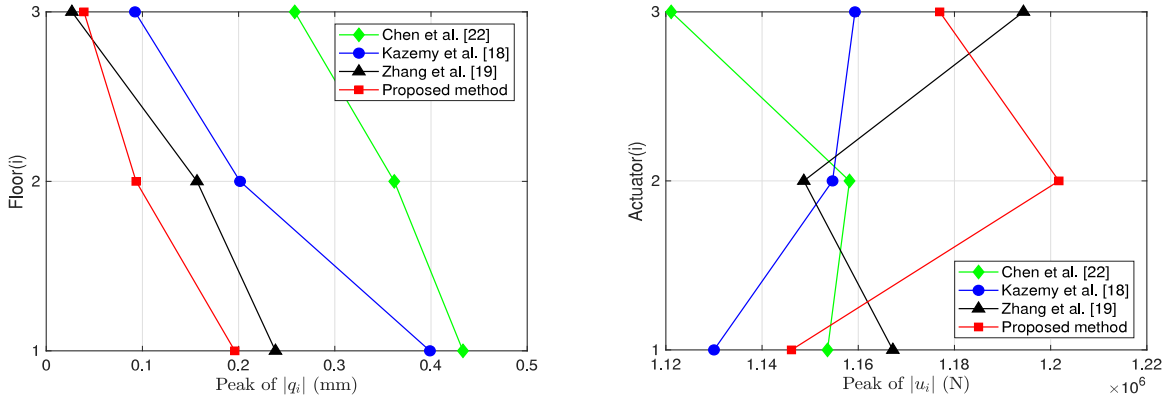

(a) (b)

Fig. 7. Comparison results for the peaks of absolute value of the (a) relative drifts $|q_i|\,(i = 1, 2, 3)$ (b) control signal $|u_i|\,(i = 1, 2, 3)$.

$$C_v = \begin{bmatrix} \frac{1}{z_{dmax}} & -\frac{1}{z_{dmax}} & 0 & 0 \\ \frac{1}{z_{pmax}} & 0 & 0 & 0 \end{bmatrix}, \qquad C_y = \begin{bmatrix} 1 & 0 & 0 & 0 \\ 0 & 1 & 0 & 0 \end{bmatrix},$$

where z_{dmax} is the maximum deflection between the AMD and the platform deck, and z_{pmax} is the maximum deviation of the platform. These limits are assumed to be $z_{dmax} = 25$ m and $z_{pmax} = 0.2$ m. For designing the controller, the values $u_{\max} = 7.6 \times 10^6$, $\varpi_1 = 0.25$, and $\varpi_2 = 5$ are considered, based on the parameters given in [35]. For the external disturbance, a wave force has been generated and shown in Fig. 9, based on JONSWAP model [38]. The dynamic output feedback controller gain matrices obtained by the proposed algorithm in the second iteration are as follows:

$$A_c = \begin{bmatrix} 6.7385 & -53.24 & 73.373 & -75.844 \\ 0.90973 & -16.033 & 16.179 & -18.314 \\ 0.38187 & -2.1075 & 1.4078 & -0.71247 \\ 0.026967 & 0.029572 & -1.8 & -0.76372 \end{bmatrix},$$

$$B_c = 10^4 \times \begin{bmatrix} -40.009 & 5.0811 \\ -87809 & 1.4810 \\ -9876.5 & 0.1965 \\ 0.2064 & -0.0052961 \end{bmatrix},$$

$$D_c = \begin{bmatrix} 5225.3 & -663.1 \end{bmatrix},$$

$$C_c = \begin{bmatrix} -0.10145 & 0.72814 & -0.96248 & 1.0034 \end{bmatrix}.$$

The closed-loop displacements and accelerations of the platform deck under this controller and three other controllers presented in [35,36], and [39] are shown in Figs. 10 and 11, respectively. These figures indicate that not only the peak of displacement, but also the peak of acceleration of the platform under the proposed controller is less than those obtained by other methods. At the same time, the constraints with z_{dmax}, z_{pmax}, and u_{max} are met, too, as it is shown in Figs. 12 and 13. It is worth noting that control signal generated by the proposed controller is smaller than the method introduced in [35], while its performance is much better. For quantitative comparison between the results, define the following parameters:

$$M_d = \max\{|x_1(t)|, t \in [0, S_t]\}, \quad J_d = \sqrt{\frac{1}{S_t}\int_0^{S_t} x_1^2(t)dt},$$

$$M_v = \max\{|x_3(t)|, t \in [0, S_t]\}, \quad J_v = \sqrt{\frac{1}{S_t}\int_0^{S_t} x_3^2(t)dt},$$

$$M_a = \max\{|\dot{x}_3(t)|, t \in [0, S_t]\}, \quad J_a = \sqrt{\frac{1}{S_t}\int_0^{S_t} \dot{x}_3^2(t)dt},$$

$$M_u = \max\{|u(t)|, t \in [0, S_t]\}, \quad J_u = \sqrt{\frac{1}{S_t}\int_0^{S_t} u^2(t)dt},$$

where S_t is the simulation time. These parameters are depicted in Table 2 for all the controllers. One can see that the obtained result has better performance compared with the other published methods while the peak of control signal and energy consumption is better than in [35] and [39], though somewhat worse than in [36] and [13]. The latter is explained by the fact that the performance of the control is measured by the penalty output only.

5. Conclusion

The design problem of FF $\mathcal{H}_\infty$ control for linear systems was addressed in this article. In order to meet practical requirements, some hard constraints of the physical system and the actuator limitation was considered in the dynamic output feedback

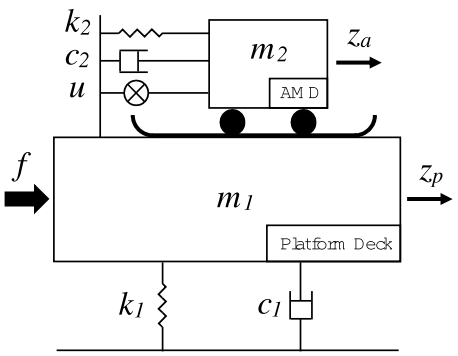

Fig. 8. Offshore steel jacket platform simplified model [35].

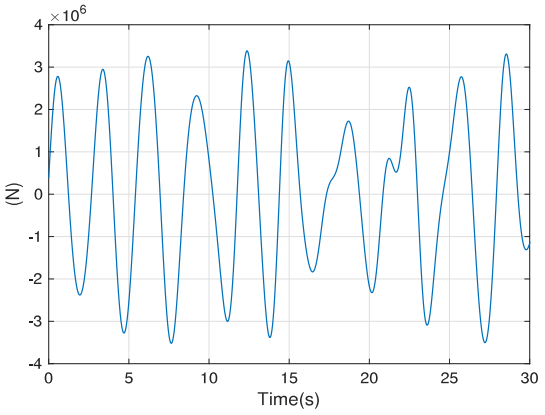

Fig. 9. Wave force generated on the basis of JONSWAP model [38].

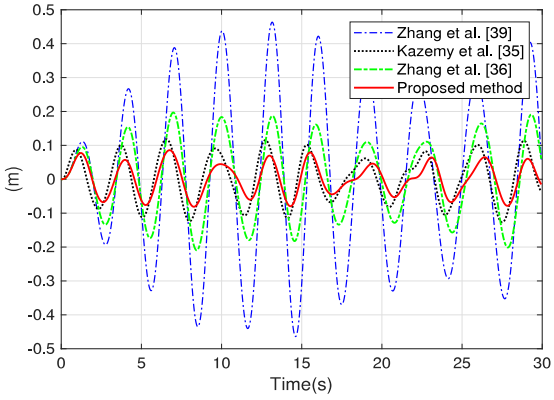

Fig. 10. Displacement of the platform deck.

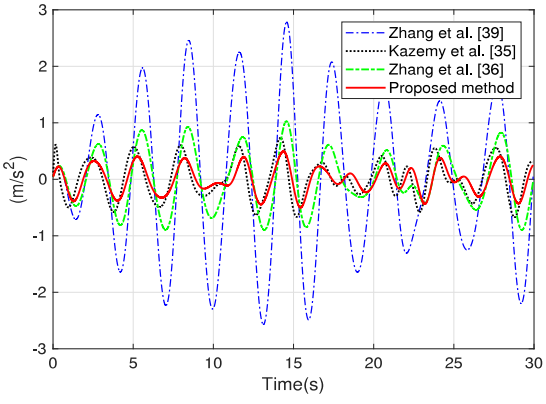

Fig. 11. Acceleration of the platform deck.

Table 2
Quantitative comparison between different controllers.

Method	M_d (m)	M_v (m/s)	M_a (m/s^2)	M_u (10^6 N)	J_d (m)	J_v (m/s)	J_a (m/s^2)	J_u (10^5 N)
No control	0.8373	1.7687	3.8246	–	0.4686	0.9551	1.929	–
[39]	0.4641	0.9975	2.7896	5.3181	0.2514	0.5112	1.3520	29.196
[13]	0.2107	0.4413	1.0434	1.2952	0.1150	0.2345	0.4992	7.1400
[36]	0.2093	0.4386	1.0313	1.2901	0.1143	0.2331	0.4946	7.0770
[35]	0.1271	0.2913	0.7359	2.9959	0.0691	0.1479	0.3403	11.6200
Proposed	0.0857	0.2067	0.5011	2.5591	0.0452	0.0984	0.2335	9.8300

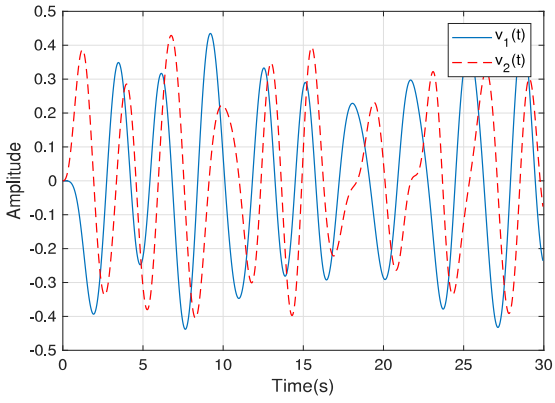

Fig. 12. Plotting $v(t)$ under the proposed controller.

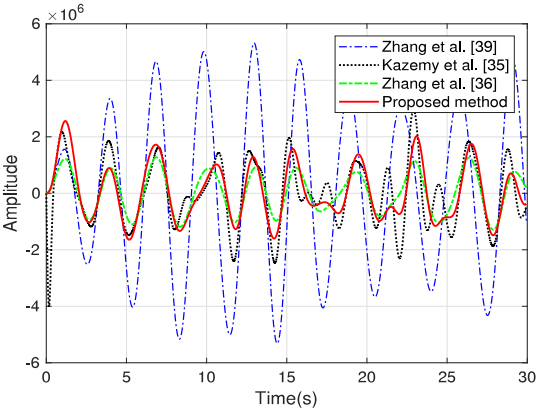

Fig. 13. Control signal generated by different controllers.

controller design. After deriving sufficient conditions on FF $\mathcal{H}_\infty$-stability based on gKYP lemma, an algorithm of finitely many steps was given to determine the dynamic output feedback with suboptimal $\mathcal{H}_\infty$-norm bound. A seismic-excited building and an offshore platform were utilized for case studies. The simulation of the behaviour of the closed-loop systems with the designed controllers showed that the proposed method was more effective than other published methods.

Declaration of competing interest

The authors declare that they have no known competing financial interests or personal relationships that could have appeared to influence the work reported in this paper.

References

[1] Francis BA. A course in $\mathcal{H}_\infty$ control theory. Berlin; New York: Springer-Verlag; 1987.
[2] Doyle JC, Glover K, Khargoneker PP, Francis BA. State-space solutions to standard $\mathcal{H}_2$ and $\mathcal{H}_\infty$ control problems. IEEE Trans Automat Control 1989;34(8):831–47.
[3] Glover K, Doyle JC. State-space formulae for all stabilizing controllers that satisfy an $\mathcal{H}_\infty$-norm bound and relations to relations to risk sensitivity. Syst Control Lett 1988;11(3):167–72.
[4] Petersen IR, Ugrinovskii VA, Savkin VA. Robust control design using $\mathcal{H}_\infty$ methods. Springer Science & Business Media; 2012.
[5] Xie L, de Souza CE. Robust $\mathcal{H}_\infty$ control for linear systems with norm-bounded time-varying uncertainty. IEEE Trans Automat Control 1992;37(8):1188–91.
[6] Isidori A, Astolfi A. Disturbance attenuation and $\mathcal{H}_\infty$-control via measurement feedback in nonlinear systems. IEEE Trans Automat Control 1992;37(9):1283–93.
[7] Chen B-S, Tseng Ch-Sh, Uang H-J. Mixed $\mathcal{H}_2/\mathcal{H}_\infty$ fuzzy output feedback control design for nonlinear dynamic systems: an lmi approach. IEEE Trans Fuzzy Syst 2000;8(3):249–65.
[8] Choi HH, Chung MJ. Memoryless $\mathcal{H}_\infty$ controller design for linear systems with delayed state and control. Automatica 1995;31(6):917–9.
[9] Sun Y, Li N, Shen M, Wei Zh, Sun G. Robust $\mathcal{H}_\infty$ control of uncertain linear system with interval time-varying delays by using Wirtinger inequality. Appl Math Comput 2018;335:1–11.
[10] Xiang W, Lam J, Li P. On stability and $\mathcal{H}_\infty$ control of switched systems with random switching signals. Automatica 2018;95:419–25.
[11] Souza AG, Souza LCG. Design of a controller for a rigid-flexible satellite using the h-infinity method considering the parametric uncertainty. Mech Syst Signal Process 2019;116:641–50.
[12] Zhao W, Fan M, Wang Ch, Jin Zh, Li Y. $\mathcal{H}_\infty$/extension stability control of automotive active front steering system. Mech Syst Signal Process 2019;115:621–36.
[13] Kazemy A. Robust mixed $\mathcal{H}_\infty$/passive vibration control of offshore steel jacket platforms with structured uncertainty. Ocean Eng 2017;139:95–102.
[14] Sakthivel R, Selvaraj P, Mathiyalagan K, Park JH. Robust fault-tolerant $\mathcal{H}_\infty$ control for offshore steel jacket platforms via sampled-data approach. J Franklin Inst B 2015;352(6):2259–79.
[15] Wang G, Chen Ch, Yu Sh. Robust non-fragile finite-frequency $\mathcal{H}_\infty$ static output-feedback control for active suspension systems. Mech Syst Signal Process 2017;91:41–56.
[16] Li H, Jing X, Karimi HR. Output-feedback-based $\mathcal{H}_\infty$ control for vehicle suspension systems with control delay. IEEE Trans Ind Electron 2014;61(1):436–46.
[17] Rigatos G, Siano P, Raffo G. A nonlinear h-infinity control method for multi-dof robotic manipulators. Nonlinear Dynam 2017;88(1):329–48.
[18] Kazemy A, Zhang X-M, Han Q-L. Dynamic output feedback control for seismic-excited buildings. J Sound Vib 2017;411:88–107.
[19] Zhang H, Wang R, Wang J, Shi Y. Robust finite frequency $\mathcal{H}_\infty$ static-output-feedback control with application to vibration active control of structural systems. Mechatronics 2014;24(4):354–66.
[20] Iwasaki T, Hara Sh. Generalized KYP lemma: Unified frequency domain inequalities with design applications. IEEE Trans Automat Control 2005;50(1):41–59.
[21] Pipeleers G, Vandenberghe L. Generalized KYP lemma with real data. IEEE Trans Automat Control 2011;56(12):2942–6.
[22] Chen Y, Zhang W, Gao H. Finite frequency $\mathcal{H}_\infty$ control for building under earthquake excitation. Mechatronics 2010;20(1):128–42.
[23] Xu J, Shi P, Lim Ch-Ch, Cai Ch. A descriptor-system approach for finite-frequency $\mathcal{H}_\infty$ control of singularly perturbed systems. Inform Sci 2016;370:79–91.
[24] Li X-J, Yang G-H. Adaptive $\mathcal{H}_\infty$ control in finite frequency domain for uncertain linear systems. Inform Sci 2015;314:14–27.
[25] Wang R, Jing H, Yan F, Karimi HR, Chen N. Optimization and finite-frequency $\mathcal{H}_\infty$ control of active suspensions in in-wheel motor driven electric ground vehicles. J Franklin Inst B 2015;352(2):468–84.
[26] Xu J, Cai Ch, Cai G, Zou Y. Robust $\mathcal{H}_\infty$ control for miniature unmanned aerial vehicles at hover by the finite frequency strategy. IET Control Theory Appl 2016;10(2):190–200.
[27] Sun W, Gao H, Kaynak O. Finite frequency $\mathcal{H}_\infty$ control for vehicle active suspension systems. IEEE Trans Control Syst Technol 2011;19(2):416–22.
[28] Wang C, Li H, Chen Y. $\mathcal{H}_\infty$ Output feedback control of linear time-invariant fractional-order systems over finite frequency range. IEEE/CAA J Autom Sin 2016;3(3):304–10.

[29] Wang R, Jing H, Karimi HR, Chen N. Robust fault-tolerant $\mathcal{H}_\infty$ control of active suspension systems with finite-frequency constraint. Mech Syst Signal Process 2015;62–63:341–55.
[30] Li H, Jing X, Karimi HR. Output-feedback-based $\mathcal{H}_\infty$ control for vehicle suspension systems with control delay. IEEE Trans Ind Electron 2014;61(1):436–46.
[31] Zheng X, Zhang H, Wang Z. Dynamic output-feedback control for active vehicle suspension systems subject to actuator faults in finite frequency domain. Proceedings of the 36th Chinese control conference 2017;9413–8.
[32] Gahinet P, Apkarian P. A linear matrix inequality approach to $\mathcal{H}_\infty$ control. Internat J Robust Nonlinear Control 1994;4(4):421–48.
[33] Skelton RE, Iwasaki T, Grigoriadis DE. A unified algebraic approach to control design. CRC Press; 1997.
[34] Löfberg J. Yalmip : A toolbox for modeling and optimization in matlab. In: Proceedings of the CACSD conference. 2004, page (http://users.isy.liu.se/johanl/yalmip/) [Accessed on 18 December 2017].
[35] Kazemy A, Lam J, Li X. Finite-frequency $\mathcal{H}_\infty$ control for offshore platforms subject to parametric model uncertainty and practical hard constraints. ISA Trans 2018;83:53–65.
[36] Zhang B-L, Tang G-Y. Active vibration $\mathcal{H}_\infty$ control of offshore steel jacket platforms using delayed feedback. J Sound Vib 2013;332(22):5662–77.
[37] Kazemy A. $\mathcal{H}_\infty$ Filter design for offshore platforms via sampled-data measurements. Smart Struct Syst 2018;21(2):187–94.
[38] Hasselmann K, Barnett TP, Bouws E, Carlson H, Cartwright DE, Enke K, et al. Measurements of wind wave growth and swell decay during the joint north sea wave project (JONSWAP). Ergänzungsheft Dtsch Hydrographischen Z Reihe 1973;8(12):95.
[39] Zhang BL, Han QL, Zhang XM. Event-triggered $\mathcal{H}_\infty$ reliable control for offshore structures in network environments. J Sound Vib 2016;368:1–21.